Mikada, H., Moore, G.F., Taira, A., Becker, K., Moore, J.C., and Klaus, A. (Eds.)
Proceedings of the Ocean Drilling Program, Scientific Results Volume 190/196

8. Data Report: The Relation between Physical Properties and Grain-Size Variations in Hemipelagic Sediments from Nankai Trough[1]

Joan F. Steurer[2] and Michael B. Underwood[2]

ABSTRACT

We present the results of grain-size analysis performed on hemipelagic sediment from Sites 1173, 1174, 1175, and 1177 at the Nankai Trough. Analyses of the <63-µm fraction were performed with a laser particle counter, and results were converted to equivalent settling diameters by means of an empirical regression with data from pipette analysis. The relations among grain size, porosity, bulk density, void ratio, and moisture content are influenced by the increasing compaction of sediment with depth as well as facies changes. Thus, departures of bulk density and porosity from normal compaction trends cannot be attributed to grain size on the basis of our laboratory results.

INTRODUCTION

Grain-size analysis is useful for characterizing a wide variety of physical properties of marine sediment. Grain size and sorting affect porosity and permeability (e.g., Boggs, 1995; Fetter, 2001), and they are also related to the geotechnical properties of sediment. For instance, the relation between void ratio and applied effective stress can be strongly influenced by grain size, as are physiochemical and mechanical factors during consolidation. Clays, especially highly colloidal ones, experience greater reduction in void ratio under a given increase in effective stress than do silty clays or silts (Mitchell, 1993). The presence of abun-

[1]Steurer, J.F., and Underwood, M.B., 2003. Data report: The relation between physical properties and grain-size variations in hemipelagic sediments from Nankai Trough. *In* Mikada, H., Moore, G.F., Taira, A., Becker, K., Moore, J.C., and Klaus, A. (Eds.), *Proc. ODP, Sci. Results,* 190/196, 1–25 [Online]. Available from World Wide Web: <http://www-odp.tamu.edu/publications/190196SR/VOLUME/CHAPTERS/210.PDF>. [Cited YYYY-MM-DD]
[2]101 Geological Sciences, University of Missouri, Columbia MO 65211, USA. Correspondence author: **jfs349@mizzou.edu**

Initial receipt: 18 November 2002
Acceptance: 18 June 2003
Web publication: 11 November 2003
Ms 190SR-210

dant clay can also inhibit crushing of diatoms and calcareous tests during consolidation, which contributes to the maintenance of porosity (Hein, 1991). Grain size also affects Atterberg limits, bulk density, shear strength, permeability, and pore pressure transients in response to cyclic loading (Hein, 1991).

Leg 190 of the Ocean Drilling Program (ODP) targeted the Nankai convergent margin, southwest Japan, for the purpose of understanding the complex relations among deformation, diagenesis, and fluid flow. To this end, we clustered samples for studies of mineralogy next to those for geotechnical and geochemical analyses. The first objective of this report is to summarize the grain-size data for the sample clusters so that the results of geotechnical tests can be interpreted more effectively. A second objective is to document a method for using a laser particle counter for performing grain-size analysis with fine-grained sediment.

GEOLOGIC CONTEXT

The Nankai Trough is an active clastic-dominated convergent margin where the Philippine Sea plate is being subducted beneath the Eurasian plate. Drilling during Leg 190 targeted two transects (Fig. F1). The Muroto Transect included a reference site (Site 1173) that penetrated the prism's toe (Site 1174) and three sites on the landward slope (including Site 1175). Site 1177 was drilled as the reference site for the Ashizuri Transect.

At Sites 1173 and 1174, we cored five major lithostratigraphic units (Figs. F2, F3) (Shipboard Scientific Party, 2001b, 2001c). The trench-wedge facies consists mainly of thick sand and silt turbidites with interspersed hemipelagic mud. The upper Shikoku Basin facies consists mainly of hemipelagic mudstone and volcanic ash. The lower Shikoku Basin facies consists of hemipelagic mudstone with scattered carbonate-cemented nodules and siliceous mudstone. A volcaniclastic unit of variegated mudstone lies atop pillow basalt (Shipboard Scientific Party, 2001b, 2001c).

We cored three units at Site 1175 (Fig. F4). The upper slope-basin facies consists of hemipelagic mud rich in nannofossils, thin silty and sandy turbidites, and volcanic ash. The middle slope-basin facies consists of muddy sand, thin silty and sandy turbidites, hemipelagic mud, and volcanic ash. The strata below 300 meters below seafloor (mbsf) contain carbonate-poor hemipelagic mud, sandy and silty turbidites, and gravelly mudstone (Shipboard Scientific Party, 2001d).

The uppermost 300 m was not cored at Site 1177, and the topmost unit encountered is the upper Shikoku Basin facies. Beneath that facies are the lower Shikoku Basin hemipelagic facies and the lower Shikoku Basin turbidite facies, where sand, silty sand, and hemipelagic mudstone are interspersed with scattered gravel, mudstone-clast conglomerate, and siliceous and carbonate-cemented claystone. The lowermost sedimentary unit is the volcaniclastic-rich facies, which consists of silty claystone, vitric mudstone, and sandy and silty beds (Shipboard Scientific Party, 2001e).

F1. Nankai Trough study area, p. 14.

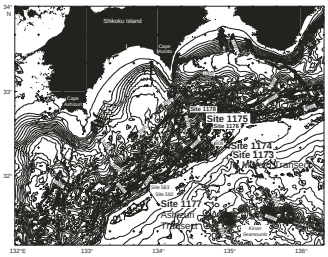

F2. Sand, silt, and clay and grain size, Site 1173, p. 15.

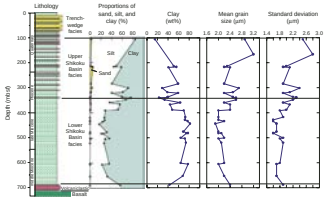

F3. Sand, silt, and clay and grain size, Site 1174, p. 16.

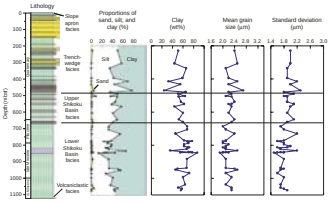

F4. Sand, silt, and clay and grain size, Site 1175, p. 17.

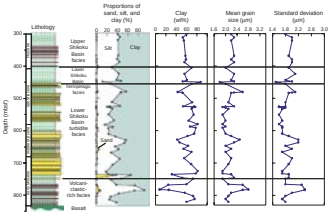

METHODS

Sample Preparation

Because the whole-round samples for geotechnical tests were taken from hemipelagic sediments and the muddy intervals of the turbidite-rich facies, the grain-size samples are exclusively fine grained. Samples were freeze-dried and weighed. They were then placed in a beaker and treated with 3% H_2O_2 for a minimum of 24 hr until digestion of organic matter had ceased. Samples were then dispersed with 250 mL of 4 g/L sodium hexametaphosphate (Calgon) for a minimum of 24 hr and further dispersed via 10 min of exposure in an ultrasonic bath. Highly indurated mudstones were exposed to gentle crushing and longer treatment periods with frequent stirring.

We separated the <63-µm fraction by wet sieving. Fluid volume of the silt and clay suspension was then brought to 500 mL with deionized, distilled water and vigorously agitated. For 45 of the samples, a 20-mL aliquot was extracted from a depth of 20 cm. We corrected for the presence of Calgon in each aliquot by subtracting 0.04 g, and the result was multiplied by 25 in order to obtain a weight for the fine-grained fraction without organic matter.

We then reagitated and removed a few milliliters of sediment suspension with a disposable pipette. This suspension was further diluted in deionized water, and a few drops of the diluted suspension were placed in a clear glass bottle of filtered deionized water, taking care to ensure thorough mixing of the suspension throughout the process. This dilute suspension was scanned with the laser particle counter as described below in order to distinguish between the abundances of clay- and silt-sized particles.

Spectrex Laser Particle Counter

Operation and Output

In order to estimate the percent clay vs. percent silt in the <63-µm fraction, we used a Spectrex PC-2000 laser particle counter (LPC). The LPC measures the cross-sectional dimension of particles by light scattering. A laser diode rotates at a constant rate, illuminating a volume of water in which sediment is suspended. As the beam strikes a particle, the light is scattered, and the scattered light is collected by a photodetector. This causes an electrical pulse in the connected preamplifer, and the amplitude and width of the pulse is a function of the grain size (Spectrex Corporation, 1998). The LPC is rapid; it is possible to measure the grain-size distribution in 30 s.

Typical output from the LPC may be seen in Table T1. The output includes the number of counts per cubic centimeter that fall into each size bin. Sixteen bins, plus a <1- and a >17-µm bin, are included, although other binning options are available for analysis of coarser-grained sediment. The >17-µm bin is designated as the "overflow bin" and labeled "9999" (Table T1). Bins are 1 µm in width, and the number in the "Size" column refers to the lower limit of the range. The Supercount software (version 6.7; Spectrex Corporation, 1998) that accompanies the device also automatically computes the percentages of the total counts, the cross-sectional area, and mass as well as the parts per million in each bin, but these calculations are based on assumptions of

T1. Supercount software output, p. 21.

concentration, dilution, and particle density as well as shape, which the user must input.

Supercount also calculates the mean grain size and the standard deviation of grain-size distribution. This calculation includes two important assumptions. First, the lower limit of a given bin is taken as the size of all particles in that bin. Using the midpoint of the bin is more representative of the entire bin width than the lower limit (e.g., McBride, 1971). Second, the <1-µm bin is not considered in the calculations. Since the bins are 1 µm in width, these approximations may not significantly affect the accuracy of statistics for coarser-grained distributions. Because a large proportion of the particles fall into the <1-µm bin, eliminating this bin would introduce large errors.

We calculated mean size as

$$\bar{x} = \frac{\sum_{i=1}^{N} C_i m_i}{C_t}$$

where

$\bar{x}$ = mean grain size,
C_i = counts per cubic centimeter in the *i*th bin,
m_i = midpoint size of the *i*th bin,
N = number of bins, and
C_t = total counts per cubic centimeter of sized grains.

We used only the sized grains in calculating C_T because the grains in the overflow bin (9999) are undifferentiated by size. These grains may be any size over 17 µm, which made choosing a midpoint size for this bin impossible. In practice, however, the average counts per cubic centimeter in the overflow bin were <1%, so the associated error is small.

The standard deviation of the grain-size distribution is typically used as a measure of sorting (e.g., Boggs, 1995). We calculated standard deviation, σ, by

$$\sigma = \sqrt{\frac{\sum_{i=1}^{N} C_i (m_i - \bar{x})^2}{C_t}} .$$

We used 0.75 µm as the midpoint of the 0- to 1-µm bin because of the inability of the laser particle counter to detect particles <0.5 µm.

Development of Scanning Protocol

We developed a system for running the LPC measurements with fine-grained materials based on repeated testing of standards included with the laser particle counter and natural samples that had been separated by centrifuge. The procedure differs from that recommended by the Spectrex Corporation's instruction manual (Spectrex Corporation, 1998). These choices are summarized in Table T2 and briefly explained below.

T2. Settings for the Spectrex LPC, p. 22.

The method of agitation is to gently invert the bottle for 30 s at a rate of ~1 cycle every 2 s then allow 15 s of rest prior to scanning in order to eliminate air bubbles. More vigorous agitation introduces excessive air, and less vigorous agitation or a longer rest period allows the larger particles to settle to the bottom prior to scanning. We found this method

of agitation preferable to using the magnetic stirrer with which the LPC is equipped. Introducing the stirring magnet into the bottle resulted in a larger number of background counts, especially in the finer size bins. Furthermore, the particles counted are too small to settle to the bottom of the water column during the scan time of 30 s, so the use of the stirring device is unnecessary.

The instrument's threshold controls the smallest particle size to be counted. The wavelength of the light (670.8 nm) limits the smallest resolvable particle to 0.5 µm, so we placed the threshold at this level (threshold = 7). Lower thresholds result in rapid counting in the absence of any particles because of the effects of light scattering (Spectrex Corporation, 1998). To avoid the effects of light interference at this threshold, it is necessary to shield the exposed upper half of the bottle during scanning. The LPC is equipped with a light shield because ambient light causes interference, but light filtering through the bottle top still causes rapid counting in the <1-µm bin if a secondary shield is not in place. This problem is eliminated by inverting a cardboard box and placing it over the bottle.

The most troublesome parameter is sediment concentration. When particles interact or drift too close to one another, the LPC measures them as a single large particle. If the concentration is too great, the number of counts in the smaller size bins drops to zero and the resulting grain-size distribution is too coarse. Furthermore, the count rate appears to limit the ability of the instrument to a maximum of ~1000 particles/cm³. Using a restricted range of counts per cubic centimeter is therefore critical. We compared distribution by weight yielded by pipette analysis to counts yielded by LPC scan and found that concentrations near 800 counts/cm³ had the greatest similarity. We also used a centrifuge to make three size splits, <2, 2–4, and >4–8 µm. Using these fractions of equivalent spherical size, we scanned various concentrations with the LPC and calculated the percentage of counts in the expected ranges. The percentage of particles being counted in the expected range sharply decreased with concentration >750 counts/cm³ for the <2-µm fraction but sharply increased with concentration >800 counts/cm³ for the 4- to 8-µm fraction. In order to balance these effects, we chose a concentration of 750–800 counts/cm³ based on similarities between LPC and both pipette and centrifuge results. With concentrations >900 counts/cm³, the percentage of particles <4 µm in diameter dropped to zero. We interpret this effect to be due to physical interactions between particles. These higher concentrations, though within the range recommended by the manufacturer, can therefore cause the LPC to grossly underrecord the percentage by counts of clay-sized particles.

In order to evaluate the precision of the entire procedure, we randomly selected 24 samples for duplicate runs, wherein the agitation, ultrasonic vibration, dilution, and scanning were repeated. Correlation between repeat runs is 0.84. An F-test reveals that the variances of the two groups of runs are the same, and a Student's t-test demonstrates that the means of the two groups are equal above the 95% probability level (Fig. F5). Twelve runs of the same suspension show that the standard deviation of percentage of counts per cubic centimeter <4 µm = 1.5% ± 2.5%.

F5. LPC, p. 18.

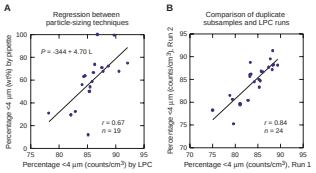

Correlation with Pipette Analysis

In order to standardize the Spectrex laser method to weight percent by settling methods, we correlated the LPC results with the results of pipette analysis. The goal of this analysis is to determine the percent by weight of clay- vs. silt-sized particles in the <63-µm fraction, with the clay-sized fraction defined as the Stokes' spherical settling equivalent of all particles <4 µm in diameter.

For constructing the correlation function, the <4-µm fractions of 20 samples were extracted with the pipette method (e.g., Galehouse, 1971). The same samples were analyzed with the LPC prior to pipetting. Linear regression between the two data sets yields an empirical function for converting the LPC counts to equivalent Stokes' settling diameter (Fig. F5). The correlation coefficient for the two data sets is 0.67, which is significant at the 95% confidence interval. The function is

$$P = -344 + 4.70L,$$

where

P = weight percent of <4-µm particles by the pipette method and
L = percent of total counts per cubic centimeter of particles <4 µm by the LPC method.

Our comparison shows that the fraction of counts per cubic centimeter by LPC using our method overestimates the weight fraction of clay as compared to spherical settling equivalents.

A second comparison focused on the <2-µm Stokes' size fraction for the purpose of estimating the absolute abundance of various clays examined by X-ray diffraction analysis. However, regression between the percent of particles <2 µm by counts and the weight percent of particles <2 µm by the pipette method was insignificant at the 95% confidence interval (r = 0.44). The lower correlation coefficient is most likely due to the inability of the LPC to resolve particles <0.5 µm in diameter. Furthermore, very small particles are affected by Brownian movement of molecules in the fluid, so Stokes' Law becomes invalid for particles <0.5 µm in size (Galehouse, 1971). Particles in the size range below the resolution of the LPC may constitute a significant portion of the sediment; pipette analysis on two randomly selected samples suggests that the <0.5-µm fraction may be ~20% by weight of the fine fraction and 65% of the <2-µm fraction for some samples.

Previous Tests of Laser Counters

Previous studies have demonstrated that when compared to other methods, laser diffraction size analysis is generally accurate, especially when compared to methods based on the measurement of size rather than Stokes' settling. For example, Hall (1988) found no significant differences between results from the Spectrex LPC and the Coulter counter. Similarly, in comparing laser particle counters manufactured by Coulter and Malvern to the Coulter counter TA1, Loizeau et al. (1994) found that results from the laser devices are in good agreement with those of the Coulter counter. However, laser counter results are less similar to settling methods, especially when substantial amounts of clay-sized particles are present. Hall (1988) found that grain-size distribution results by the Spectrex LPC showed a shift toward coarser grains

relative to pipette results. Damm (1990) similarly demonstrated a shift of particle size distributions toward coarser grains using the Malvern laser counter relative to results from pipette and Sedigraph techniques, both of which are settling methods.

The agreement between laser particle counter results and those of settling methods decreases when substantial amounts of clay-sized particles are present (Loizeau et al., 1994; Singer, 1988). One reason for differences in the results is a fundamental difference in the dimension measured by laser particle counters and that measured by settling analysis. Whereas the laser particle counter measures the cross-sectional surface of the particles, settling methods measure the weight percent of spherical settling equivalent sizes. Both methods are affected in different ways by particle shape. With a platy particle, the orientation of the particle at the time of measurement affects the LPC results. Nonsphericity as well as particle density also affects settling rates during pipette or similar analyses. Damm (1990) concluded that since platy particles do not conform to ideal spherical settling behavior, the laser particle results are more representative of the true grain-size distribution when platy particles are present.

A second reason for decreased agreement between laser particle sizing and settling velocity methods is the lower limit of size resolution of the laser counter (Loizeau et al., 1994; Singer et al., 1988). The laser device simply does not detect particles below the resolution limit. The pipette technique is also unreliable for measuring the weight percent of particles <0.5 µm in diameter, but rather than eliminating the particles from analysis as does the laser particle analyzer, the unresolvable fraction is incorporated into the smallest fraction extracted (Galehouse, 1971).

Konert and Vandenberghe (1997) compared the laser particle sizing technique to the pipette technique and showed that the <2-µm grain size as defined by the pipette method corresponds most closely to the fraction of particles <8 µm in dimension by counts as defined by the laser sizing technique. Using this larger fraction as the clay fraction would allow comparisons between the two techniques. Their scanning electron microscopy examination of <2-µm equivalent settling diameter particles revealed that these particles are up to 10 µm in the long dimension for platy clay mineral grains but with a thickness of <1 µm. They demonstrated mathematically that grains of these dimensions were the volume equivalent of <2-µm spheres, and their empirical results are in good agreement with this theory.

Singer et al. (1988) cited physical interactions between clay particles as a reason for underreporting of the abundance of <4-µm particles by the Malvern laser counter relative to particle-settling techniques. When two particles drift too near one another, the laser particle counter records them as a single large particle, leading to the underreporting of the percentage of counts of finer particles and overreporting of coarser particles. Our technique for fine-grained materials, in contrast to some previous studies, overpredicts the proportion of clay-sized particles relative to pipette analysis. Our strict control on the number of counts per cubic centimeter, in order to avoid physical particle interactions as described previously, is likely the cause of this contrast.

Moisture and Density

Shipboard data include porosity measurements by the moisture and density techniques (Blum, 1997). Most of the samples for grain-size

analysis are within 20 cm of physical property samples. We used the porosity, bulk density, void ratio, and water content of the nearest sample to explore the relation between those properties and grain size.

RESULTS

Grain Size

Table T3 shows the percentage of sand-, silt-, and clay-sized particles by weight (equivalent setting diameter) for the four sites studied. Where measured, the percentage of organic matter by weight is also shown. Typical total losses through digestion by H_2O_2 were ~2% by weight, although this amount also includes any small losses during the sieving process. In cases in which the loss through digestion was not measured, the nonsand portion of the sediment is assumed to be 100% minus the percent by weight of sand. Table T3 also shows the percentage of counts per cubic centimeter <4 µm, as measured by the LPC, as well as the mean particle size and standard deviation of distribution calculated from the LPC results. Figures F2, F3, and F4 show the variations of grain-size classes with depth for Sites 1173, 1174, and 1177, respectively.

Figures F2, F3, and F4 also show the percentage of clay by weight as determined by the empirical correlation of LPC measurements to pipette analysis and mean grain size and sorting. We correlated each of these parameters to moisture and density properties for each site, and representative plots of these regressions may be seen in Figure F6. Because of the low weight percentages of sand and organic matter, the percentage of silt is approximately equal to 100% minus the percentage of clay and is therefore not displayed in the illustrations.

T3. Grain size results, p. 23.

F6. Bulk density, porosity, void ratio, and water content, p. 19.

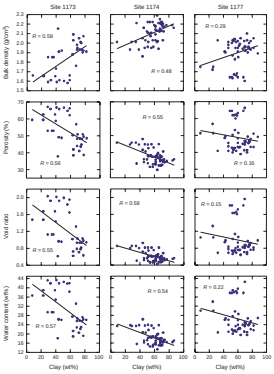

Site 1173

Grain-size data were collected from the upper and lower Shikoku Basin facies at this site, with a single datum for the volcaniclastic facies. As expected for hemipelagic sediments, the proportion of sand is low, averaging 2% by weight in the upper Shikoku Basin facies and <1% in the lower Shikoku Basin facies. Mudstones from the lower Shikoku Basin facies contain more clay-sized particles than mud from the upper Shikoku Basin facies, ranging from 30% to 80% by weight. Except for two very low values, the average percentage of clay by weight for the upper Shikoku Basin facies is 41%, and for the lower Shikoku Basin facies it is 64%. This increase in the abundance of clay-sized particles coincides with an increase in total clay minerals at the boundary between the upper and lower Shikoku Basin facies (Shipboard Scientific Party, 2001b).

The average mean particle size as calculated from LPC for samples from the upper Shikoku Basin facies is 2.6 µm and 2.2 µm for samples from the lower Shikoku Basin facies. The average standard deviation of particle size for samples from the upper Shikoku Basin facies is 2.2 µm and 1.8 µm for the lower Shikoku Basin facies.

Site 1174

Grain-size data were collected from the hemipelagic sediments of the trench-wedge, upper, and lower Shikoku Basin facies at Site 1174. The relative proportion of sand is low. The trench-wedge samples have an

average of 1% of sand by weight, the upper Shikoku Basin facies shows an average of 2%, and the lower Shikoku Basin facies contains an average of 1%. The increase of clay-sized particles with depth is more subtle at Site 1174 than at Site 1173 but nonetheless present. Clay increases from ~50% at the top of the trench-wedge facies to ~65%–70% at 850 mbsf. Below this depth, the percent clay remains at ~60% to the base of the unit. This increase in clay-sized particles coincides with an increase of total clay minerals (Shipboard Scientific Party, 2001c). The average percent clay by weight for the trench-wedge facies is 44%, for the upper Shikoku Basin facies it is 56%, and for the lower Shikoku Basin facies it is 65%.

The average mean particle size is 2.4 µm for the trench-wedge facies, 2.3 µm for the upper Shikoku Basin facies, and 2.2 µm for the lower Shikoku Basin facies. The average standard deviation is equal to 2.1 µm for samples from the trench wedge, 2.0 µm for samples from the upper Shikoku Basin facies, and 1.7 µm for samples from the lower Shikoku Basin facies.

Site 1175

The four samples of sediment from Site 1175 are generally richer in sand than those from the other sites, ranging from 2% to 8%. Silt ranges from 32% to 55%, and clay ranges from 38% to 64%. The mean size of the <63-µm fraction is 2.3 µm, and the average standard deviation for these samples is 2.0 µm.

Site 1177

We collected grain-size data from the hemipelagic sediments of all units at this site. The upper Shikoku Basin facies has average proportions of <1%, 42%, and 57% for sand, silt, and clay-sized particles by weight, respectively. The lower Shikoku Basin hemipelagic facies contains averages of 1% sand-, 39% silt-, and 59% clay-sized particles, although only four samples from this unit were analyzed. Mud from the lower Shikoku Basin turbidite facies contains an average of 1% sand, 34% silt, and 63% clay, exclusive of one anomalously sandy sample that came from a turbidite. The volcaniclastic-rich facies contains averages of 2% sand-, 47% silt-, and 51% clay-sized particles, although the data are scattered with the percent clay ranging from 10% to 75%.

The average mean grain size for the upper Shikoku Basin facies is 2.3 µm, 2.2 µm for the lower Shikoku Basin hemipelagic facies, 2.1 µm for the lower Shikoku Basin turbidite facies, and 2.3 µm for the volcaniclastic-rich facies. The average standard deviations are 1.9 µm for the upper Shikoku Basin facies, 2.0 µm for the lower Shikoku Basin hemipelagic facies, 1.8 µm for the lower Shikoku Basin turbidite facies, and 2.0 µm for the volcaniclastic-rich facies.

Moisture and Density

As may be seen in Figure F6, bulk density seems to increase with weight percent clay. Porosity, void ratio, and water content decrease with weight percent clay. Nearly identical trends are also seen with mean grain size and standard deviation. The correlations between physical properties and grain-size distribution are stronger for samples from Sites 1173 and 1174 than for those from Site 1177. For Site 1173, correlation coefficients between weight percent clay, mean grain size, or

standard deviation and porosity, bulk density, void ratio, or water content range from 0.53 to 0.58. For Site 1174, correlation coefficients range from 0.48 to 0.58. For Site 1177, correlation coefficients range from 0.15 to 0.36.

Results from analyses of variance demonstrate that all correlations between all three grain-size measures and properties for Sites 1173 and 1174 are statistically significant above the 95% confidence interval. For Site 1177, only correlations between average grain size and standard deviation with the properties of bulk density and water content, as well as percent clay with bulk density, were significant at the 95% confidence interval.

DISCUSSION

Our results for grain sizes and clay abundances are comparable to those of other workers studying hemipelagic sediment. Diemer and Forsythe (1995), using both the Spectrex laser particle counter and a rapid sediment analyzer, found that silty clays from the inner trench slope of the Chile margin have an average size of ~2.0–2.4 µm. Cavin et al. (2000), using a Sedigraph, found that hemipelagic mud from the Cascadia Basin typically contains 60%–85% clay and the mean size ranges from 1 to 4 µm.

Grain-size variations in sediment from the Muroto Transect show subtle trends with depth, and these trends are at in part a function of the original depositional environment. The lower Shikoku Basin facies contains no turbidites, so grain sizes tend to be smaller and better sorted. Precipitation of authigenic clay may also contribute to the decreased particle sizes with depth because of the dissolution of disseminated volcanic ash as it alters to clay. At Site 1177, the relations of mean grain size and sorting with lithologic unit are less clear. The upper Shikoku Basin samples from this site show a higher average mean grain size than either the lower Shikoku Basin hemipelagic or turbidite facies, and the sorting in terms of standard deviation is similar in both the upper and lower units. For samples from Site 1177, the weight percentage of clay only shows a slight difference between the upper and lower Shikoku Basin units, with the upper Shikoku Basin facies samples containing only 5% less clay by weight than the lower Shikoku Basin units. It is difficult to resolve any differences between the lower Shikoku Basin hemipelagic and turbidite facies because of the small number of samples analyzed.

Changes in moisture content and bulk density also show depth-related trends. At the Muroto Transect, sediment follows a complicated compaction trend with depth. The upper Shikoku Basin facies, for example, shows nearly constant porosity with depth. This anomalous porosity-depth relation is also seen in the upper Shikoku Basin facies at Site 1177 (Shipboard Scientific Party, 2001a, 2001b, 2001c). The compaction trend with depth is also irregular at Site 1177, but porosity generally decreases with depth (Shipboard Scientific Party, 2001c). Related trends are also noted in bulk density, which generally increases with depth (Shipboard Scientific Party, 2001b, 2001c, 2001e).

Figure F7 shows the relation of weight percent clay with porosity for Sites 1173, 1174, and 1177, and the lithologic units are highlighted in each plot. It is clear that the decrease in porosity coincides with increasing depth. A similar depth dependency occurs for bulk density, void ratio, and water content. The correlations between grain size and physical

F7. Porosity vs. clay, p. 20.

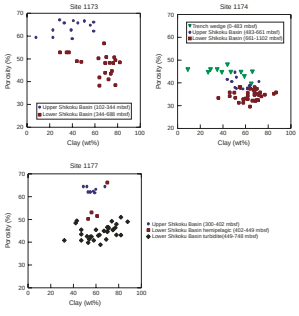

properties (Fig. F6), therefore, are largely the result of the combined effects of downward-fining stratigraphy and increasing sediment compaction with depth.

SUMMARY

This report presents a summary of grain-size data for samples of hemipelagic sediment from Sites 1173, 1174, 1175, and 1177. These data consist of the weight percents of sand, silt, and clay, mean grain size, and standard. We also show the values of porosity, bulk density, void ratio, and water content as measured shipboard for nearby sample intervals. These data provide useful information for physical properties and geotechnical experiments, especially those which will attempt to examine the lithologic controls on the mechanical properties or fluid-sediment interactions.

At Sites 1173 and 1174, bulk density appears to increase with weight percent clay, whereas porosity, void ratio, and water content appear to decrease with weight percent clay. These relations, however, are strongly influenced by a combination of facies changes and increasing compaction with depth. Thus, the true effect of grain size as a primary control on physical properties has been masked by spatial and temporal variations in compaction. Correlations between grain-size parameters and index properties are even weaker at Site 1177. This may be due to differences in compaction within the heterogeneous lithologies of the lower Shikoku Basin turbidite facies.

New laboratory procedures have been developed for using the Spectrex laser particle counter with fine-grained sediment. We used an empirical correlation with pipette analysis to convert laser particle counter results to weight percent of spherical equivalent settling.

ACKNOWLEDGMENTS

We thank Captain Tom Ribbens, the crew, technicians, and fellow scientists aboard *JOIDES Resolution* for their dedicated assistance during ODP Leg 190. We also thank an anonymous reviewer for his helpful suggestions. Ron Sammons and Eric Grabowski assisted in the laboratory. This research used samples provided by the Ocean Drilling Program, which is sponsored by the U.S. National Science Foundation and participating countries under management of Joint Oceanographic Institutions, Inc. Funding was provided by a Schlanger Ocean Drilling Fellowship to J. Steurer and the U.S. Science Support Program (grant F001281 to M. Underwood).

REFERENCES

Blum, P., 1997. Physical properties handbook: a guide to the shipboard measurement of physical properties of deep-sea cores. *ODP Tech. Note,* 26 [Online]. Available from World Wide Web: <http://www-odp.tamu.edu/publications/tnotes/tn26/INDEX.HTM>. [Cited 2002-05-15]

Boggs, S., 1995. *Principles of Sedimentology and Stratigraphy* (2nd ed.): Upper Saddle River, NJ (Prentice-Hall, Inc.).

Cavin, A. Underwood, M.B., Fisher, A.T., and Johnston, K.A., 2000. Relations between textural characteristics and physical properties of sediments in northwestern Cascadia Basin. *In* Fisher, A.T., Davis, E.E., and Escutia, C. (Eds.), *Proc. ODP, Sci. Results,* 168: College Station, TX (Ocean Drilling Program), 67–84.

Damm, E., 1990. Laser diffraction: a new method for grain size analysis of sediments. *Z. Geol. Wiss.*, 18:249–253.

Diemer, J.A., and Forsythe, R., 1995. Grain-size variations within slope junction facies recovered from the Chile margin triple junction. *In* Lewis, S.D., Behrmann, J.H., Musgrave, R.J., and Cande, S.C. (Eds.), *Proc. ODP, Sci. Results*, 141: College Station, TX (Ocean Drilling Program), 79–94.

Fetter, C.W., 2001. *Applied Hydrogeology* (4th ed.): Upper Saddle River, NJ (Prentice-Hall, Inc.).

Galehouse, J.S., 1971. Sedimentation analysis. *In* Carver, R.E. (Ed.), *Procedures in Sedimentary Petrology:* New York (Wiley), 69–94.

Hall, M.J., 1988. Comparison of Spectrex laser particle counter with Coulter counter and pipette sizing methods. *Geol. Soc. Am. Bull.*, 20:24. (Abstract)

Hamilton, E.L., 1976. Variations of density and porosity with depth in deep-sea sediments. *J. Sediment. Petrol.,* 46:280–300.

Hein, F.J., 1991. The need for grain size analyses in marine geotechnical studies. *In* Syvitski, J.P.M. (Ed.), *Principles, Methods, and Application of Particle Size Analysis:* New York (Cambridge Univ. Press), 346–362.

Konert, M., and Vandenberghe, J., 1997. Comparison of laser grain size analysis with pipette and sieve analysis: a solution for the underestimation of the clay fraction. *Sedimentology,* 44:523–535.

Loizeau, J.L., Arbouille, D., Santiago, S., and Vernet, J.P., 1994. Evaluation of wide range laser diffraction grain size analyser for use with sediments. *Sedimentology,* 41:353–361.

McBride, E.F., 1971. Mathematical treatment of size distribution data. *In* Carver, R.E. (Ed.), *Procedures in Sedimentary Petrology:* New York (Wiley).

Mitchell, J.K., 1993. *Fundamentals of Soil Behavior* (2nd ed.): New York (Wiley).

Shipboard Scientific Party, 2001a. Leg 190 summary. *In* Moore, G.F., Taira, A., Klaus, A., et al., *Proc. ODP, Init. Repts.,* 190: College Station TX (Ocean Drilling Program), 1–87.

————, 2001b. Site 1173. *In* Moore, G.F., Taira, A., Klaus, A., et al., *Proc. ODP, Init. Repts.,* 190, 1–147 [CD-ROM]. Available from: Ocean Drilling Program, Texas A&M University, College Station TX 77845-9547, USA.

————, 2001c. Site 1174. *In* Moore, G., Taira, A., Klaus, A., et al., *Proc. ODP, Init. Repts.,* 190, 1–149 [CD-ROM]. Available from: Ocean Drilling Program, Texas A&M University, College Station TX 77845-9547, USA.

————, 2001d. Site 1175. *In* Moore, G.F., Taira, A., Klaus, A., et al., *Proc. ODP, Init. Repts.,* 190, 1–92 [CD-ROM]. Available from: Ocean Drilling Program, Texas A&M University, College Station TX 77845-9547, USA.

————, 2001e. Site 1177. *In* Moore, G.F., Taira, A., Klaus, A., et al., *Proc. ODP, Init. Repts.,* 190, 1–91 [CD-ROM]. Available from: Ocean Drilling Program, Texas A&M University, College Station TX 77845-9547, USA.

Singer, J.K., Anderson, J.B., Ledbetter, M.T., McCave, I.N., Jones, K.P.N., and Wright, R., 1988. An assessment of analytical techniques for the size analysis of fine-grained sediments. *J. Sediment. Petrol.,* 58:534–543

Spectrex Corporation, 1998. *Instruction Manual for Spectrex Laser Particle Counter Model PC-2000*. Available from: Spectrex Corporation, 3580 Haven Avenue, Redwood City CA 94063, USA.

Figure F1. Map of Nankai Trough study area showing ODP and DSDP sites. Grain-size data are for Sites 1173, 1174, and 1175 on the Muroto Transect and Site 1177 on the Ashizuri Transect (after Shipboard Scientific Party, 2001a).

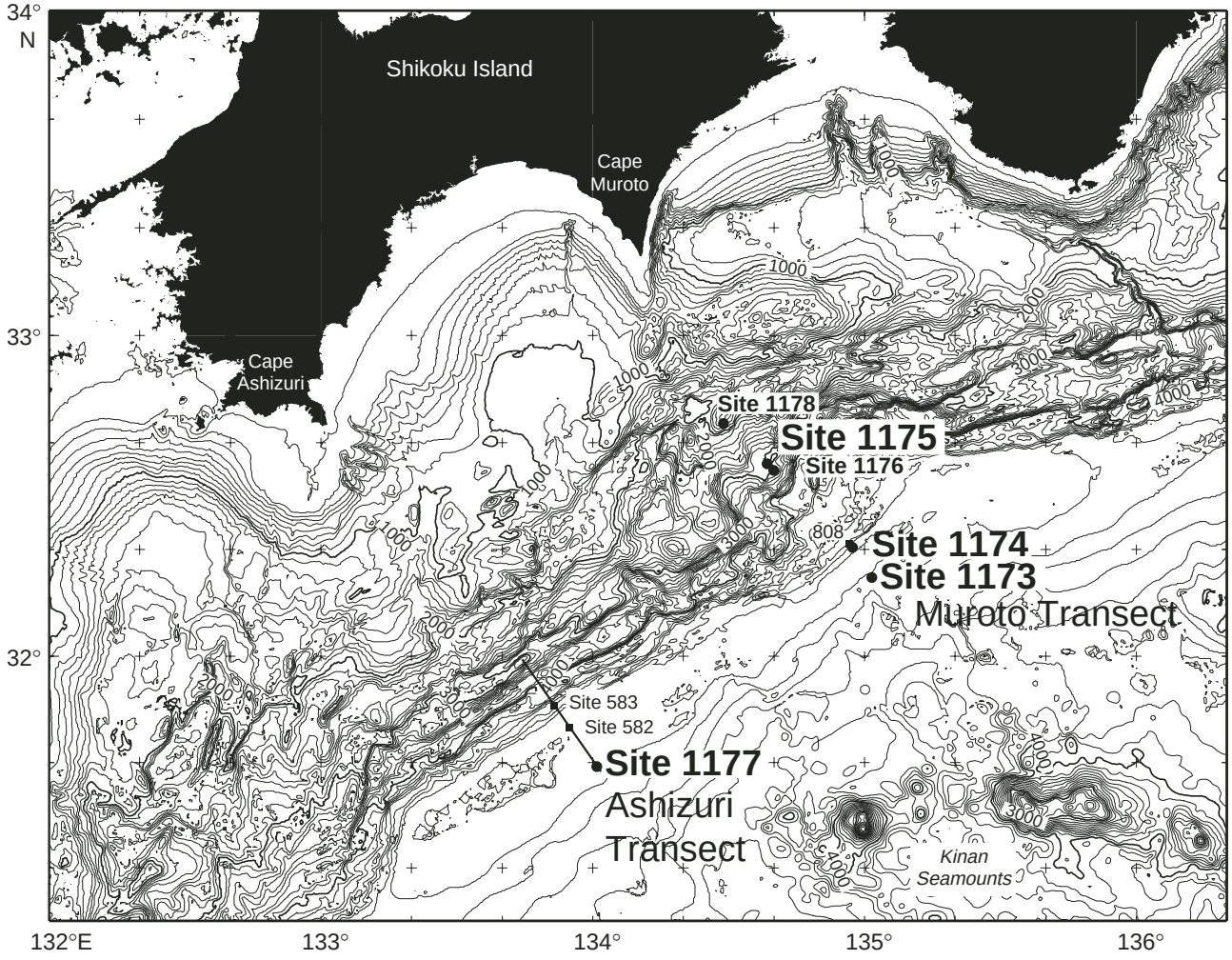

Figure F2. Lithostratigraphy, proportions of sand, silt, and clay by weight, mean grain size, and standard deviation of grain size with respect to depth for Site 1173. Sand was measured by sieve analysis. Other sizes were measured with a laser particle counter. The percent of particles <4 µm was converted to weight percent clay by use of an empirical correlation with settling analysis. Mean grain size and standard deviation were calculated from laser particle counter results. Horizontal lines show facies boundaries (after Shipboard Scientific Party, 2001b).

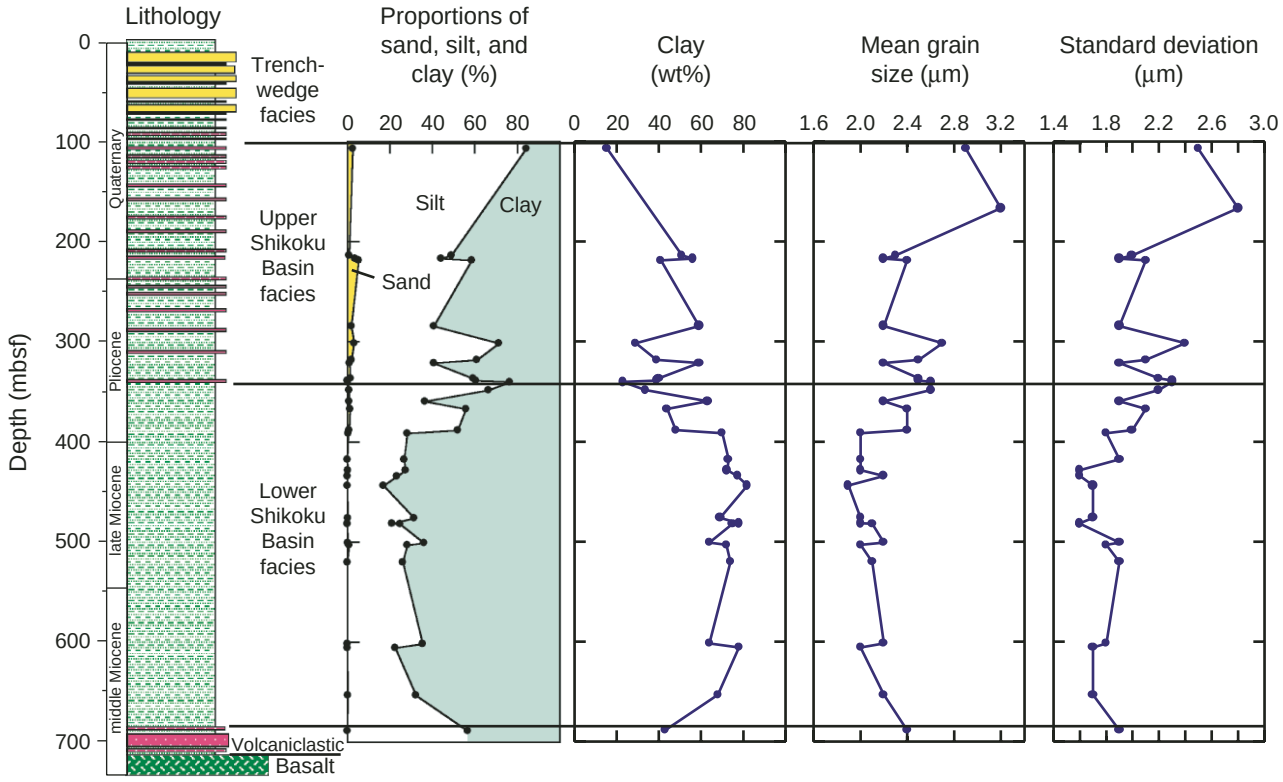

Figure F3. Lithostratigraphy, proportions of sand, silt, and clay by weight, mean grain size, and standard deviation of grain size with respect to depth for Site 1174. Sand was measured by sieve analysis. Other sizes were measured with a laser particle counter. The percent of particles <4 µm was converted to weight percent clay by use of an empirical correlation with settling analysis. Mean grain size and standard deviation were calculated from laser particle counter results. Horizontal lines show facies boundaries (after Shipboard Scientific Party, 2001c).

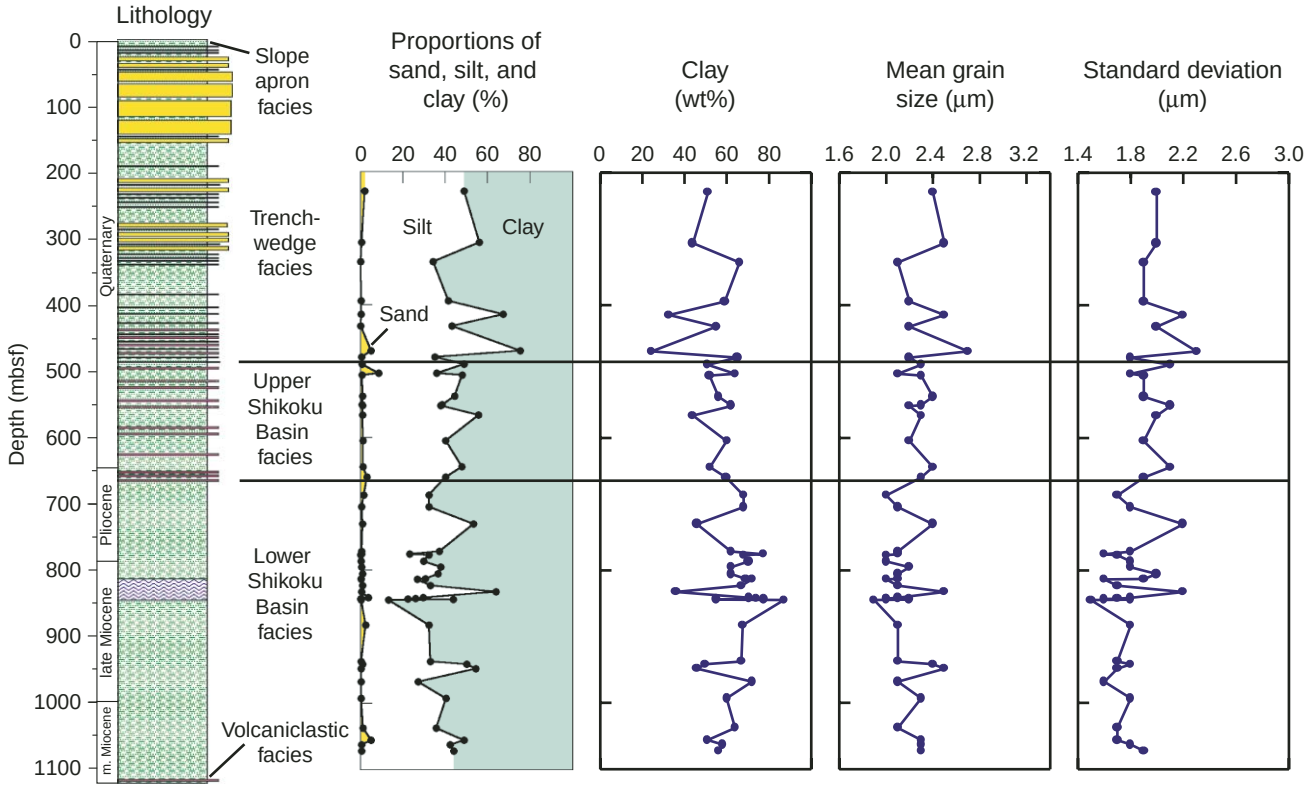

Figure F4. Lithostratigraphy, proportions of sand, silt, and clay by weight, mean grain size, and standard deviation of grain size with respect to depth for Site 1177. Sand was measured with sieve analysis. Other sizes were measured with a laser particle counter. The percent of particles <4 µm was converted to weight percent clay by use of an empirical correlation with settling analysis. Mean grain size and standard deviation were calculated from laser particle counter results. Horizontal lines show facies boundaries (after Shipboard Scientific Party, 2001c).

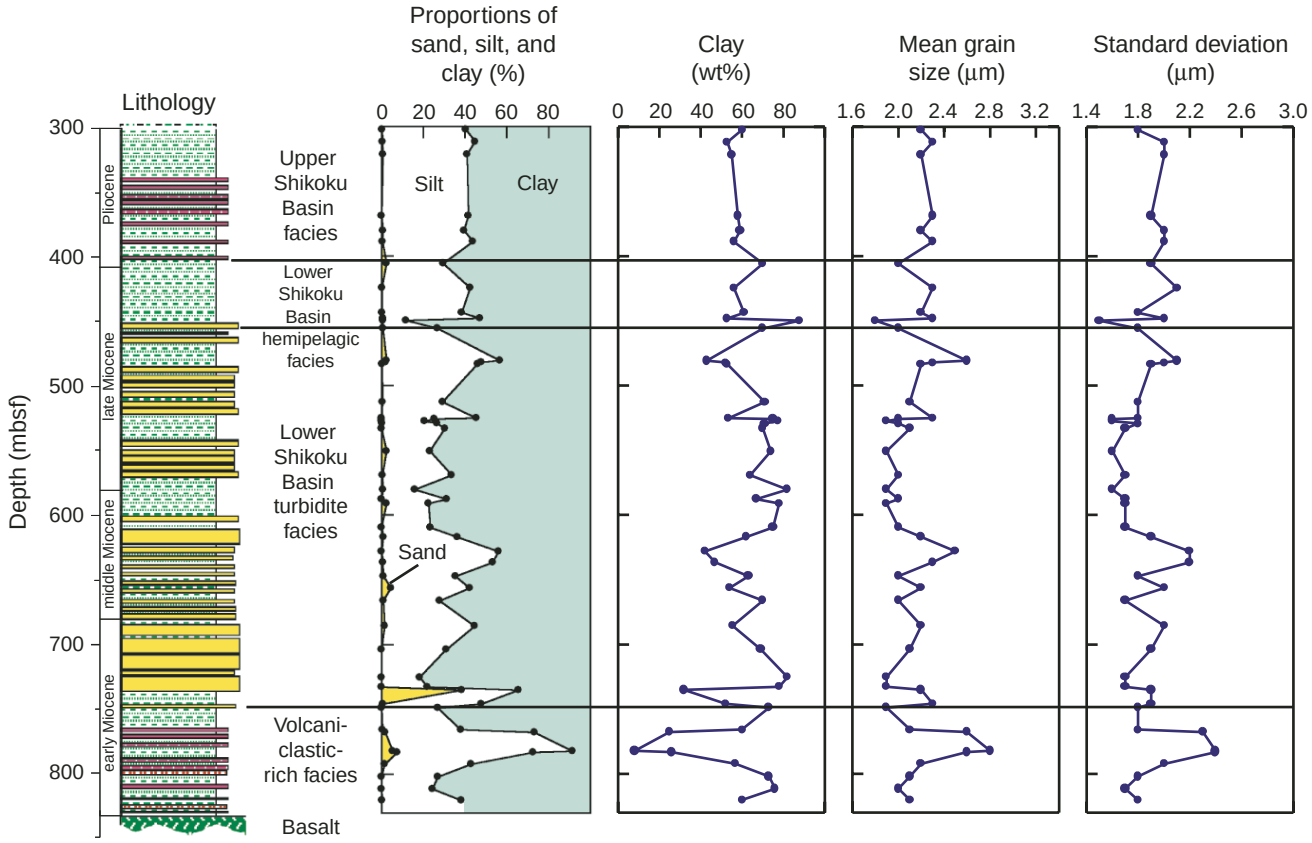

Figure F5. A. Linear regression between percent clay-sized particles as measured by laser particle counter (LPC) and weight percent clay-sized particles as measured by the pipette technique. **B.** Comparison of repeated runs with the LPC on duplicate subsamples.

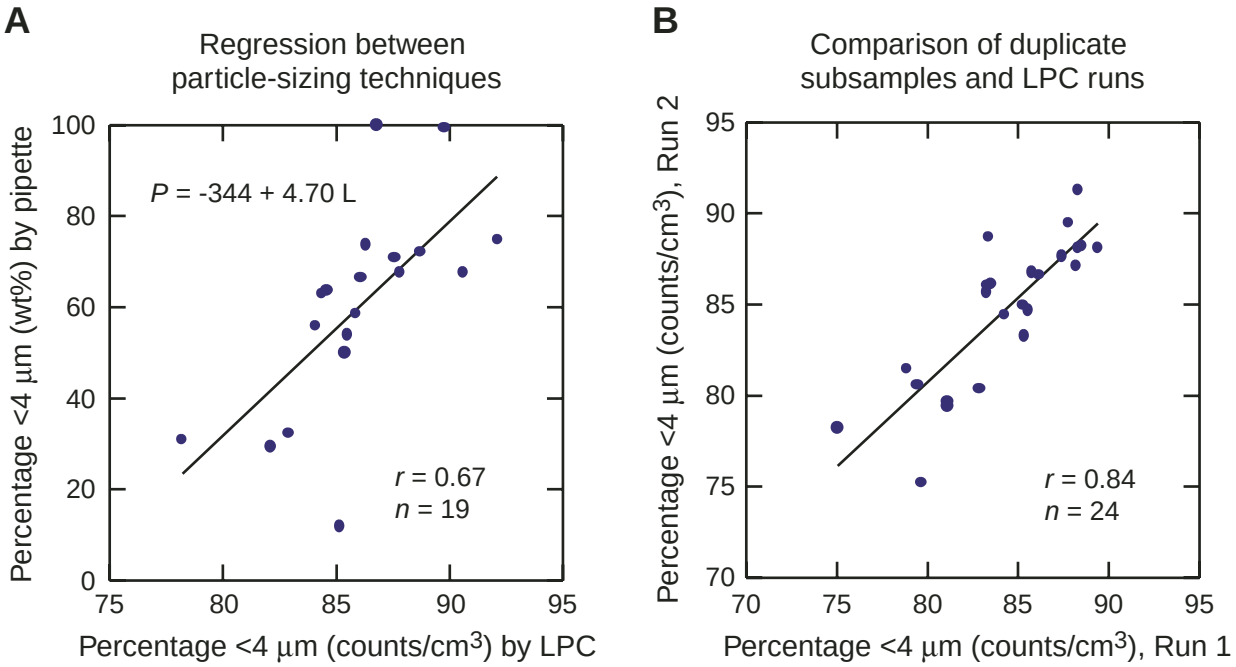

Figure F6. Linear regression of bulk density, porosity, void ratio, and water content with weight percent clay for Sites 1173, 1174, and 1177. The vertical scale is the same across each row, and the horizontal scale is the same for each plot.

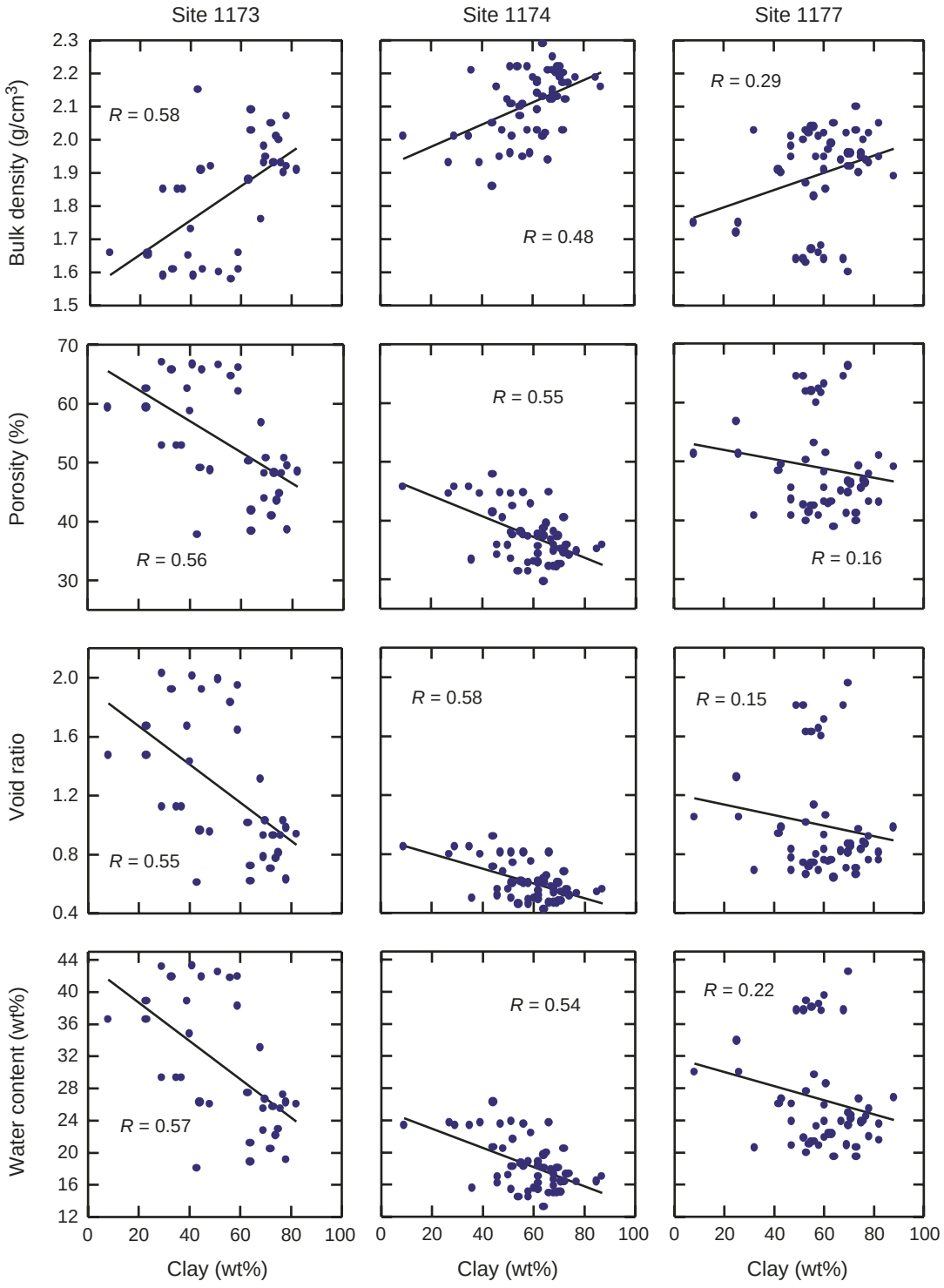

Figure F7. Porosity vs. weight percent clay for Sites 1173, 1174, and 1177. Circles = upper Shikoku Basin facies, squares = lower Shikoku Basin facies. Other facies associations are as shown.

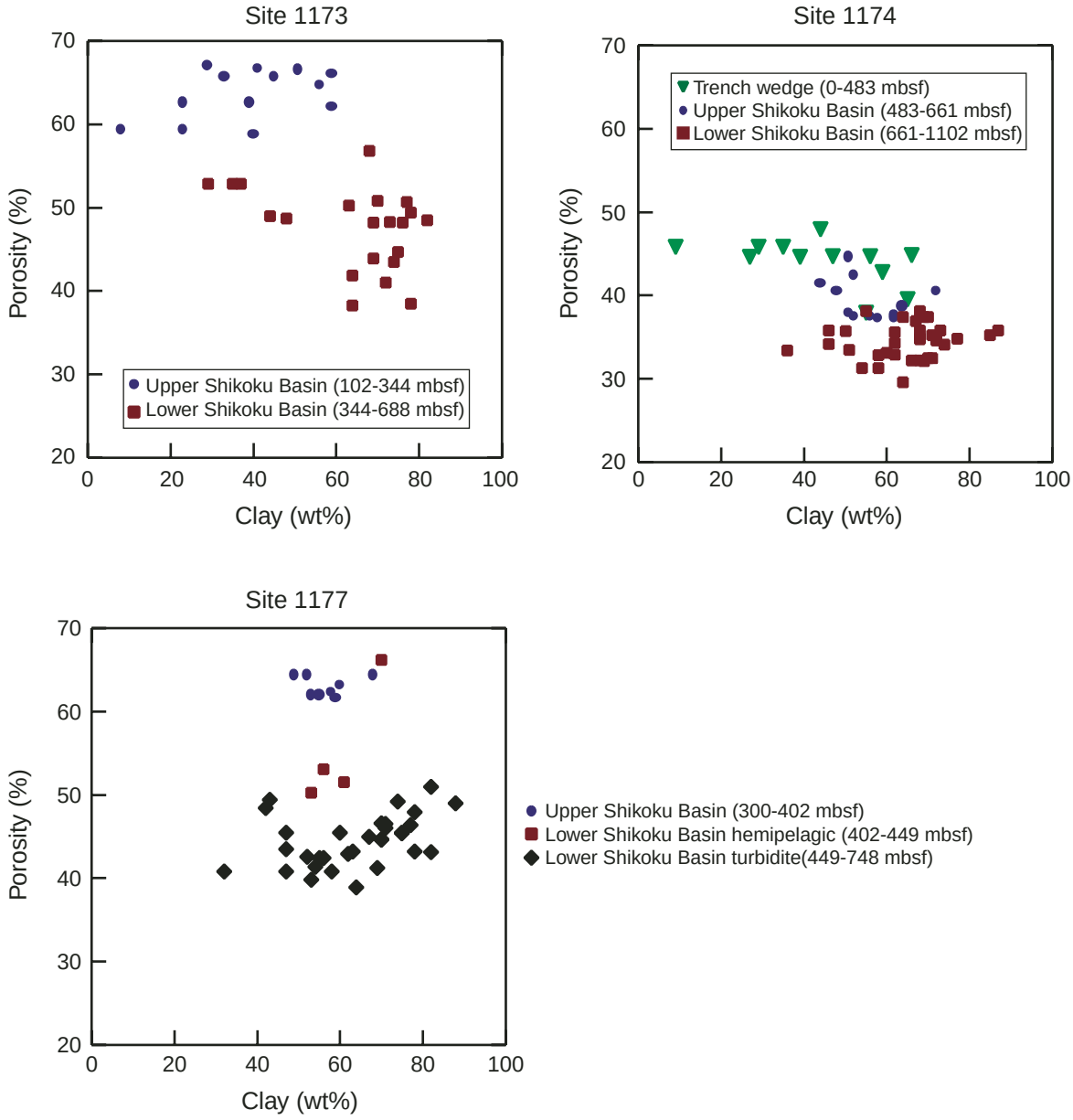

Table T1. Typical output from the Spectrex laser particle counter Supercount software.

Bin	Size (µm)	Counts	Sample (%)	Area (%)	Mass (%)	ppm
	0	274.5	34.6	0.0	0.00	0.0000
1	1	148.1	18.7	2.6	0.48	0.0002
2	2	125.3	15.8	8.7	3.23	0.0014
3	3	105.7	13.3	16.5	9.21	0.0039
4	4	59.4	7.5	16.5	12.26	0.0052
5	5	42.5	5.4	18.5	17.14	0.0072
6	6	18.5	2.3	11.6	12.91	0.0054
7	7	7.1	0.9	6.0	7.84	0.0033
8	8	4.4	0.5	4.8	7.20	0.0030
9	9	2.7	0.3	3.8	6.41	0.0027
10	10	1.6	0.2	2.8	5.27	0.0022
11	11	2.2	0.3	4.6	9.36	0.0039
12	12	0.0	0.0	0.0	0.00	0.0000
13	13	0.5	0.1	1.6	3.86	0.0016
14	14	0.5	0.1	1.9	4.82	0.0020
15	15	0.0	0.0	0.0	0.00	0.0000
16	16	0.0	0.0	0.0	0.00	0.0000
	9999	0.0	0.0	0.0	0.00	0.0000

Total counts:	793
Total ppm:	0.0422
Mean:	2.8
Standard deviation:	1.8
Dilution:	1

Notes: The size is the lower limit of each size class. Counts reports of particles <1 µm. The overflow bin (9999) contains counts of particles >17 µm. Parts per million and percent sample, area, and mass are calculated from user-input assumptions.

Table T2. Summary of procedures and settings for using the Spectrex laser particle counter with fine-grained sediment.

Procedure	Setting or technique
Threshold	<0.5 µm (setting 7)
Background	<20 counts/cm^3
Agitation	Invert bottle every 2 s for 30 s, taking care to avoid introducing air bubbles. Rest 15 s before beginning scan.
Scan time	30 s
Scan type	Normal
Filter	<1 µm to >16 µm
Concentration	700–800 counts/cm^3

Table T3. Summary of grain size results. (See table notes. Continued on next two pages.)

Core, section, interval (cm)	Depth (mbsf)	Size classes (wt%)*				Grain-size parameters†			Shipboard measurements‡			
		Sand (>63 µm)	Silt (64–4 µm)	Clay (<4 µm)	Organics	<4 µm (%)	Mean (µm)	SD (µm)	Porosity (%)	Bulk density (g/cm^3)	Void ratio	Water content (wt%)
190-1173A-												
Unit II												
12H-4, 48	107.12	3	89	8	—	75	3.0	2.7	59.4	1.66	1.47	36.6
12H-4, 48	107.12	3	74	23	—	78	2.7	2.3	59.4	1.66	1.47	36.6
18H-6, 16	166.80	1	99	0	—		3.2	2.8	67.8	1.56	2.11	42.3
23H-5, 131	213.95	1	48	51	—	84	2.3	2.0	66.6	1.60	1.99	42.5
24H-1, 123	217.37	4	41	56	—	86	2.2	1.9	64.7	1.58	1.83	41.8
24H-2, 128	218.92	5	53	41	—	83	2.4	2.1	66.7	1.59	2.01	43.3
31X-1, 131	284.55	2	39	59	—	86	2.2	1.9	66.1	1.61	1.95	42.0
32X-6, 130	301.74	3	68	29	—	80	2.7	2.4	67.0	1.59	2.03	43.2
34X-5, 54	318.48	2	53	45	—	83	2.5	2.1	65.7	1.61	1.92	41.9
34X-5, 54	318.48	2	65	33	—	80	2.5	2.2	65.7	1.61	1.92	41.9
34X-CC, 16	321.54	1	40	59	—	86	2.2	1.9	62.1	1.66	1.64	38.2
36X-4, 93	336.57	2	57	40	2	82	2.5	2.2	58.8	1.73	1.43	34.8
36X-6, 33	338.97	0	60	39	—	82	2.5	2.3	62.6	1.65	1.67	38.8
36X-CC, 21	340.16	0	73	23	4	78	2.6	2.3	62.6	1.65	1.67	38.8
190-1173A-												
Unit III												
37X-6, 35	348.59	1	62	37	—	81	2.6	2.2	52.9	1.85	1.12	29.3
37X-6, 35	348.59	1	70	29	—	79	2.6	2.2	52.9	1.85	1.12	29.3
37X-6, 35	348.59	1	65	35	—	81	2.6	2.3	52.9	1.85	1.12	29.3
38X-CC, 21	360.00	1	36	63	—	87	2.2	1.9	50.3	1.88	1.01	27.4
39X-5, 133	367.27	1	55	44	—	83	2.4	2.1	49.0	1.91	0.96	26.3
41X-7, 26	388.50	1	51	48	—	84	2.4	2.0	48.7	1.92	0.95	26.0
42X-2, 118	391.52	0	27	70	2	89	2.0	1.8	50.8	1.95	1.03	26.6
44X-CC, 27	417.79	0	27	73	—	89	2.0	1.9	48.3	1.93	0.93	25.7
46X-1, 132	428.56	0	31	69	—	88	2.0	1.8	48.2	1.93	0.93	25.5
46X-1, 132	428.56	0	23	76	—	90	2.0	1.5	48.2	1.93	0.93	25.5
46X-5, 121	434.45	0	23	77	—	90	2.2	1.6	50.7	1.90	1.03	27.3
47X-5, 130	443.74	0	17	82	1	91	1.9	1.7	48.5	1.91	0.94	26.0
51X-2, 39	476.23	0	31	69	—	88	2.0	1.7	43.9	1.98	0.78	22.7
51X-5, 118	481.52	0	21	78	1	90	2.0	1.6	49.4	1.92	0.98	26.3
51X-6, 60	482.44	0	25	75	—	89	2.1	1.6	44.7	2.00	0.81	22.9
53X-5, 128	501.02	0	36	64	—	87	2.2	1.9	41.9	2.03	0.72	21.2
53X-CC, 26	503.46	1	27	72	—	89	2.0	1.8	41.0	2.05	0.70	20.5
55X-5, 131	520.35	0	26	74	—	89	2.1	1.9	43.5	2.01	0.77	22.1
64X-2, 99	602.03	0	36	64	—	87	2.2	1.8	38.3	2.09	0.62	18.8
64X-5, 56	606.10	0	22	78	—	90	2.0	1.7	38.5	2.07	0.63	19.1
69X-4, 89	653.13	0	32	68	—	88	2.2	1.7	56.8	1.76	1.31	33.0
190-1173A-												
Unit IV												
73X-2, 86	688.70	0	56	43	1	82	2.4	1.9	37.8	2.15	0.61	18.0
190-1174B-												
Unit II												
10R-CC, 16	229.48	2	42	56	—	85	2.3	2.0	44.7	1.95	0.81	23.5
10R-CC, 16	229.48	2	51	47	—	83	2.4	2.1	44.7	1.95	0.81	23.5
18R-2, 63	306.43	1	56	44	—	83	2.5	2.0	47.9	1.86	0.92	26.3
21R-CC, 5	335.77	0	34	66	—	87	2.1	1.9	44.8	1.94	0.81	23.7
27R-3, 113	394.63	0	41	59	—	86	2.2	1.9	42.8	1.96	0.75	22.4
29R-CC, 20	414.65	0	73	27	—	81	2.4	2.0	44.6	1.93	0.80	23.7
29R-CC, 20	414.65	0	61	39	—	79	2.6	2.4	44.6	1.93	0.80	23.7
31R-3, 47	432.47	0	42	55	3	85	2.2	2.0	37.9	2.07	0.61	18.7
35R-2, 94	469.54	5	66	29	—	81	2.5	2.1	45.8	2.01	0.85	23.4
35R-2, 94	469.54	5	86	9	—	80	2.7	2.3	45.8	2.01	0.85	23.4
35R-2, 94	469.54	5	60	35	—	75	2.9	2.5	45.8	2.01	0.85	23.4
36R-2, 130	479.30	1	34	65	—	87	2.2	1.8	39.5	2.02	0.65	20.0
190-1174B-												
Unit III												
37R-3, 133	490.03	1	48	51	—	84	2.3	2.1	44.6	1.96	0.81	23.9
38R-6, 60	503.40	9	27	64	—	88	2.1	1.8	38.7	2.01	0.63	19.7
39R-1, 127	506.17	1	48	51	—	85	2.3	1.8	37.9	2.11	0.60	18.2
39R-1, 127	506.17	1	47	52	—	84	2.3	1.9	37.5	2.11	0.60	18.2
42R-3, 127	538.17	1	44	56	—	84	2.4	1.9	37.5	2.11	0.60	18.2
43R-5, 123	550.83	1	38	62	—	86	2.3	2.1	37.4	2.09	0.60	18.3
43R-6, 127	552.37	1	37	62	—	87	2.2	2.1	37.7	2.09	0.62	18.3

Table T3 (continued).

Core, section, interval (cm)	Depth (mbsf)	Size classes (wt%)*				Grain-size parameters†			Shipboard measurements‡			
		Sand (>63 µm)	Silt (64–4 µm)	Clay (<4 µm)	Organics	<4 µm (%)	Mean (µm)	SD (µm)	Porosity (%)	Bulk density (g/cm³)	Void ratio	Water content (wt%)
45R-3, 111	566.71	1	54	44	1	83	2.3	2.0	41.4	2.05	0.71	20.7
49R-3, 97	605.17	1	52	48	—	89	2.1	1.8	40.5	2.03	0.68	20.5
49R-3, 97	605.17	1	27	72	—	83	2.4	2.0	40.5	2.03	0.68	20.5
53R-3, 124	644.04	1	47	52	—	84	2.4	2.1	42.4	2.01	0.74	21.6
55R-1, 129	660.29	3	40	58	—	87	2.2	1.9	37.3	2.03	0.60	18.8
55R-1, 129	660.29	3	35	62	—	86	2.3	1.8	37.3	2.03	0.60	18.8
190-1174B-												
Unit IV												
57R-6, 135	687.15	2	31	68	—	88	2.0	1.7	38.1	2.14	0.57	17.4
59R-5, 133	704.93	1	32	68	—	88	2.1	1.8	34.9	2.15	0.54	16.6
62R-3, 92	730.42	1	52	46	1	83	2.4	2.2	34.2	2.16	0.52	16.2
66R-5, 104	771.64	0	37	62	1	87	2.1	1.8	35.6	2.14	0.55	17.0
67R-2, 96	775.40	0	23	77	—	90	2.1	1.6	34.8	2.19	0.53	16.3
67R-3, 126	777.20	—	32	68	—	88	2.0	1.7	34.7	2.25	0.53	15.8
68R-2, 134	786.74	0	29	71	—	88	2.0	1.7	32.5	2.22	0.48	15.0
68R-2, 134	786.74	0	30	70	—	88	2.1	1.8	32.5	2.22	0.48	15.0
69R-2, 127	795.14	1	37	62	—	87	2.2	1.8	32.9	2.18	0.49	15.4
70R-2, 94	805.74	1	35	62	2	87	2.1	2.0	34.3	2.17	0.52	16.2
71R-2, 1	812.89	0	30	69	—	88	2.1	1.9	32.1	2.20	0.47	14.9
71R-2, 94	813.82	0	26	72	1	89	2.0	1.6	35.1	2.20	0.54	16.3
72R-1, 117	823.37	1	33	66	—	87	2.1	1.7	32.2	2.21	0.47	14.9
72R-1, 117	823.37	1	32	68	—	88	2.2	1.8	32.2	2.21	0.47	14.9
73R-1, 80	832.60	0	63	36	1	81	2.5	2.2	33.4	2.21	0.50	15.5
73R-7, 51	841.31	4	23	73	—	89	2.1	1.7	35.8	2.12	0.56	17.3
73R-7, 51	841.31	4	29	68	—	88	2.1	1.8	35.8	2.12	0.56	17.3
74R-1, 130	842.70	0	26	74	—	89	2.0	1.7	34.1	2.17	0.52	17.4
74R-2, 58	843.48	0	29	71	—	91	1.9	1.4	35.2	2.19	0.54	16.4
74R-2, 58	843.48	0	15	85	—	88	2.0	1.8	35.2	2.19	0.54	16.4
74R-2, 125	844.15	0	43	55	2	85	2.2	1.8	38.1	2.10	0.62	18.6
74R-CC, 14	845.11	0	13	87	—	92	1.9	1.5	35.8	2.16	0.56	17.0
78R-2, 128	882.78	2	27	70	—	88	2.1	1.6	37.4	2.13	0.60	18.0
78R-2, 128	882.78	2	29	69	—	89	2.1	1.9	37.4	2.13	0.60	18.0
78R-2, 128	882.78	2	34	64	—	87	2.2	2.0	37.4	2.13	0.60	18.0
83R-7, 46	937.36	0	33	67	—	87	2.1	1.7	36.9	2.12	0.58	17.8
84R-3, 132	941.82	1	49	50	—	84	2.4	1.8	35.7	2.12	0.56	17.2
85R-1, 117	948.27	0	54	46	—	83	2.5	1.7	35.8	2.16	0.56	16.9
87R-1, 127	967.77	0	27	72	1	89	2.1	1.6	34.6	2.17	0.53	16.3
89R-6, 31	993.11	0	40	60	—	86	2.3	1.8	33.1	2.19	0.50	15.5
94R-3, 131	1037.81	1	35	64	—	87	2.1	1.7	29.6	2.29	0.42	13.2
96R-3, 17	1055.77	5	44	51	—	85	2.3	1.7	33.5	2.22	0.50	15.4
97R-1, 63	1062.93	0	42	58	—	86	2.3	1.8	32.8	2.22	0.49	15.1
98R-1, 28	1072.18	0	42	58	—	86	2.2	1.9	31.3	2.22	0.46	14.4
98R-1, 28	1072.18	0	46	54	—	85	2.3	2.0	31.3	2.22	0.46	14.4
190-1175A-												
7H-2, 135	57.49	2	40	56	2	86	2.3	2.0				
26X-3, 125	238.55	2	55	41	3	82	2.4	2.1				
31X-4, 117	288.07	2	32	64	2	87	2.1	1.8				
43X-2, 67	399.77	8	53	38	—	82	2.3	2.2				
190-1177A-												
Unit I												
1R-2, 82	302.52	0	40	60	—	86	2.2	1.8	63.1	1.64	1.71	39.5
2R-2, 111	311.81	0	44	53	2	85	2.3	2.0	61.9	1.63	1.63	38.9
3R-2, 124	321.64	1	40	55	4	85	2.2	2.0	62.0	1.67	1.63	38.1
8R-2, 53	369.03	—	42	58	—	86	2.3	1.9	62.3	1.66	1.65	38.5
9R-3, 108	380.68	1	39	59	2	86	2.2	2.0	61.6	1.68	1.60	37.6
10R-2, 148	389.08	0	51	49	—	84	2.4	2.0	64.4	1.64	1.81	37.7
10R-2, 148	389.08	0	31	68	—	84	2.3	2.1	64.4	1.64	1.81	37.7
10R-2, 148	389.08	0	48	52	—	88	2.1	1.8	64.4	1.64	1.81	37.7
190-1177A-												
Unit II												
12R-1, 44	405.74	2	27	70	1	89	2.0	1.9	66.2	1.60	1.96	42.5
13R-CC, 27	424.77	0	42	56	2	85	2.3	2.1	53.1	1.83	1.13	29.7
15R-CC, 8	443.88	0	38	61	—	86	2.2	1.8	51.5	1.85	1.06	28.5
16R-3, 119	448.09	1	46	53	0	85	2.3	2.0	50.3	1.87	1.01	27.6

Table T3 (continued).

Core, section, interval (cm)	Depth (mbsf)	Size classes (wt%)*				Grain-size parameters†			Shipboard measurements‡			
		Sand (>63 µm)	Silt (64–4 µm)	Clay (<4 µm)	Organics	<4 µm (%)	Mean (µm)	SD (µm)	Porosity (%)	Bulk density (g/cm³)	Void ratio	Water content (wt%)
190-1177A-												
Unit III												
16R-4, 144	449.84	1	11	88	—	92	1.8	1.5	49.0	1.89	0.98	26.8
17R-2, 99	455.99	1	26	70	3	89	2.0	1.8	44.7	1.96	0.81	23.3
19R-6, 42	480.72	2	55	43	—	83	2.6	2.1	49.4	1.90	0.98	26.6
19R-7, 36	482.16	2	51	47	—	83	2.4	2.2	40.8	2.01	0.69	20.8
19R-7, 36	482.16	2	40	58	—	86	2.3	1.9	40.8	2.01	0.69	20.8
20R-1, 104	483.44	0	46	53	1	85	2.2	1.9	39.8	2.03	0.66	20.0
23R-2, 42	512.95	0	29	71	—	88	2.1	1.8	46.5	1.96	0.87	24.2
24R-4, 3	525.23	0	39	60	1	83	2.4	1.8	45.5	1.95	0.83	23.9
24R-4, 3	525.23	0	52	47	1	86	2.2	1.7	45.5	1.95	0.83	23.9
24R-4, 56	525.76	0	25	75	—	89	2.0	1.6	45.5	1.95	0.83	23.9
24R-5, 128	527.68	0	21	77	2	90	1.9	1.6	46.4	1.94	0.87	24.5
24R-6, 127	529.17	0	26	71	2	89	2.0	1.8	46.0	1.92	0.85	24.6
25R-2, 130	533.20	0	30	70	—	88	2.1	1.7	46.6	1.92	0.87	24.9
27R-1, 97	550.67	2	21	74	3	90	1.9	1.6	49.2	1.90	0.97	26.6
29R-1, 34	569.24	0	33	64	3	87	2.0	1.7	38.9	2.05	0.64	19.4
30R-2, 30	580.30	1	15	82	2	91	1.9	1.6	51.0	1.95	0.81	23.5
30R-7, 29	587.79	0	31	67	2	88	2.0	1.7	45.0	1.94	0.82	23.8
31R-CC, 8	591.10	2	20	78	—	90	1.9	1.7	47.9	1.93	0.92	25.4
33R-2, 72	609.72	0	23	75	2	89	2.0	1.7	45.4	1.96	0.83	23.7
34R-CC, 13	617.23	1	35	62	2	87	2.2	1.9	42.9	1.97	0.75	22.3
35R-3, 13	628.33	0	56	42	2	82	2.5	2.2	48.4	1.91	0.94	26.0
36R-1, 24	636.54	1	53	47	—	83	2.3	2.2	43.5	1.98	0.77	26.0
37R-2, 82	647.22	1	35	63	2	87	2.0	1.8	43.2	1.99	0.76	22.3
38R-CC, 22	656.39	4	38	54	4	86	2.2	2.0	41.4	2.02	0.71	21.0
39R-1, 96	666.16	1	27	70	2	89	2.0	1.7	44.6	1.96	0.81	23.3
41R-1, 129	685.69	1	42	56	—	85	2.2	2.0	42.4	2.04	0.74	21.3
41R-1, 129	685.69	1	44	55	—	85	2.2	2.0	42.4	2.04	0.74	21.3
43R-1, 3	703.73	0	31	69	—	88	2.1	1.9	41.2	2.02	0.70	20.9
45R-2, 87	725.27	0	18	82	—	91	1.9	1.7	43.1	2.05	0.76	21.5
46R-1, 18	732.68	0	22	78	—	90	1.9	1.7	43.2	2.02	0.76	22.0
46R-2, 122	735.22	38	27	32	2	85	2.2	1.9	40.8	2.03	0.69	20.6
47R-3, 101	746.11	1	47	52	1	84	2.3	1.9	42.6	2.00	0.74	21.8
190-1177A-												
Unit IV												
47R-5, 97	749.07	0	27	73	—	89	1.9	1.8	41.2	2.03	0.70	20.7
49R-4, 20	766.00	1	37	60	2	86	2.1	1.8	48.2	1.91	0.93	25.9
49R-5, 72	768.02	2	71	25	2	79	2.6	2.3	56.8	1.72	1.32	33.9
51R-2, 23	782.33	5	86	8	—	75	2.8	2.4	51.3	1.75	1.05	30.0
51R-2, 109	783.19	7	65	26	2	79	2.6	2.4	51.3	1.75	1.05	30.0
52R-2, 56	792.36	2	41	57	—	86	2.2	2.0	59.9	1.95	0.80	23.2
53R-2, 57	801.97	0	27	73	—	89	2.1	1.8	39.8	2.10	0.66	19.4
54R-2, 48	811.48	0	24	76	—	89	2.0	1.7	46.8	2.00	0.88	24.0
55R-1, 116	820.36	0	38	60	2	86	2.1	1.8	43.2	2.02	0.76	21.9

Notes: Sand was determined by sieve analysis, organic matter was determined by loss due to digestion by H_2O_2. * = equivalent settling diameters correlated by pipette analysis. † = output from laser particle analyzer. ‡ = data from Shipboard Scientific Party (2001). SD = standard deviation.